SPECIAL TOPIC — International Conference on Nanoscience & Technology, China 2013

Templated synthesis of highly ordered mesoporous cobalt ferrite and its microwave absorption properties

Li Guo-Min(力国民)[a)b)], Wang Lian-Cheng(王连成)[a)], and Xu Yao(徐 耀)[a)†]

[a)] *Key Laboratory of Carbon Materials, Institute of Coal Chemistry, Chinese Academy of Sciences, Taiyuan* 030001, *China*
[b)] *University of Chinese Academy of Sciences, Beijing* 100049, *China*

(Received 4 September 2013; revised manuscript received 8 April 2014; published online 10 June 2014)

Based on the nanocasting strategy, highly ordered mesoporous $CoFe_2O_4$ is synthesized via the 'two-solvent' impregnation method using a mesoporous SBA-15 template. An ordered two-dimensional (*P6mm*) structure is preserved for the $CoFe_2O_4$/SBA-15 composite after the nanocasting. After the SBA-15 template is dissolved by NaOH solution, a mesoporous structure composed of aligned nanoparticles can be obtained, and the *P6mm* structure of the parent SBA-15 is preserved. With a high specific surface area (above 90 m^2/g) and ferromagnetic behavior, the obtained material shows potential in light weight microwave absorption application. The minimum reflection loss (RL) can reach −18 dB at about 16 GHz with a thickness of 2 mm and the corresponding absorption bandwidth is 4.5 GHz.

Keywords: two-solvent, mesoporous, cobalt ferrite, microwave absorption

PACS: 81.05.Zx, 81.16.–c, 77.84.–s, 75.47.Lx **DOI:** 10.1088/1674-1056/23/8/088105

1. Introduction

As an important kind of magnetic material, ferrite has been extensively studied in many fields due to its high coercivity, moderate saturation magnetization, large magnetocrystalline anisotropy, favorable mechanical and chemical stability,[1] in applications such as electrode material,[2,3] catalysis,[4,5] drug delivery,[6] electromagnetic interference,[7] etc. Moreover, it is a metal oxide, containing magnetic ions arranged in such a manner that the magnetization can be spontaneously produced and the good dielectric properties can be maintained.[8] Therefore the spinel cobalt ferrite ($CoFe_2O_4$) has been widely used as the traditional microwave absorbent. However, its high density (5.3 g/cm^3) restricts its application, and how to reduce the density becomes a key point. With the development of stealth technology, thin, light-weight, wide absorption bandwidth, and strong absorption material performance are becoming the latest design conceptions for microwave absorbents. Up to now, there have been some attempts to prepare light-weight ferrite, including ferrite hollow fibers,[9,10] hollow ferrite microspheres,[11,12] and mesoporous nickel ferrite.[13]

As is well known, soft-template and hard-template methods are the main strategies to synthesize mesoporous materials. For metal oxides, there exist some limits of controlling intermolecular forces and assembling metal precursors with the micelles for the soft-template method. Thomas *et al*.[14] reported the synthesis of periodic nanoporous cobalt ferrite (CFO) whose ordering nanostructure was partly destroyed by increasing the sintering temperature. The mesoporous Co_3O_4 with a large surface area (about 360 m^2/g) was also synthesized by using the Pluronic soft micellar templates,[15] in which the synthesis is highly sensitive to pH and temperature. Therefore, the corresponding hard-template method is a preferable way to synthesize mesoporous metal oxides/composites, such as Co_3O_4/$CoFe_2O_4$,[16] NiO,[17] Cr_2O_3, and Co_3O_4.[18] There are some reports on the mesoporous ferrite prepared with the hard-template. One-dimensional nanostructured spinel MFe_2O_4 (M = Ni, Mg, Co) was synthesized via the two-solvent method, which could guarantee the unchangeable molar ratio of precursors.[19,20] Single phase mesoporous $CoFe_2O_4$ with a high Brunauer–Emmett–Teller (BET) surface area (155.7 m^2/g) has been successfully prepared based on the nanocasting strategy using SBA-15 and KIT-6 and it is confirmed that the impregnation steps have a great influence on the structure and properties of the products.[21] Furthermore, well-ordered three-dimensional mesoporous $NiFe_2O_4$ was also synthesized by the nanocasting method with KIT-6 serving as the template, and it is revealed that the incipient impregnation method is an effective way. Importantly, the as-prepared product exhibited good microwave absorption properties.[13]

In the general process of nanocasting, the impregnation method and the solvent used are the important factors. Excessive impregnation will result in particle aggregation on the surface of the template and blocking the mosopores, and then the precursor cannot enter into the pores of the template sufficiently. On the other hand, the dispersibility of the precursor in solvent also affects the impregnation. A solvent that enhances

†Corresponding author. E-mail: xuyao@sxicc.ac.cn

© 2014 Chinese Physical Society and IOP Publishing Ltd

the capillary force of the template will be the first choice. A study by Van der Meer *et al.* has shown that the lower interfacial tension toward the water of the alkane solvents enhances the dispersion of the metal oxide precursor inside the pore network.[22] However, to the best of our knowledge, there exists no report on the electromagnetic and microwave absorption properties of ordered mesoporous crystalline $CoFe_2O_4$ prepared by a combination of the double solvent technique and incipient impregnation method. In this paper, we report the synthesis of mesoporous $CoFe_2O_4$ by the double solvent technique using a SBA-15 template. As SiO_2 is an inorganic wave-transparent material, we also investigate the role of the amorphous silica in the process of microwave absorption. The results show that these mesoporous products each have a high BET surface area and an ordered structure, which confirms that the double solvent technique is an efficient way of impregnation. Moreover, m-$CoFe_2O_4$-2 has the best microwave absorption properties and is a promising light-weight microwave absorbent.

2. Experiment

2.1. Material preparation

A typical synthesis procedure for mesoporous SBA-15 was reported as described elsewhere.[23] P123 ($EO_{20}PO_{70}EO_{20}$, Mw=5800, Aldrich, 4.0 g) was dissolved in 120 ml of 2-mol/L HCl (37 wt%) solution at room temperature. Then, tetraethyl orthosilicate (TEOS, 98%, 10.0 ml) was added into the homogeneous solution and hydrolyzed at 40 °C for 20 h under vigorous stirring. The mixture was transferred into a Teflon vessel, sealed, and heated at 90 °C for 48 h. The filtrated solid was washed with water and ethanol several times. The final sample was dried at 60 °C and calcined at 550 °C with a heating rate (Δt) of 1 °C/min in air for 5 h and the white powder SBA-15 was finally obtained.

Precursor solution was prepared by dissolving 5.82 g of $Co(NO_3)_2{\cdot}6H_2O$ and 16.16 g of $Fe(NO_3)_3{\cdot}9H_2O$ in deionized water with a 1:2 molar ratio of Co/Fe, the concentration of the mixture was about 2 mol/L. To the dispersion of n-hexane (20 ml) containing 1 g of SBA-15 in a polytetrafluoroethylene vessel, 2.5 ml of precursor solution was added dropwise. The solvent was volatilized by exposure to air whilst stirring the mixture, and then heated at 40 °C overnight, subsequently calcined at 250 °C for 5 h (Δt = 1 °C/min, air atmosphere). Afterwards, the resulting chocolate brown powder was re-impregnated and dried as described above, and calcined at 800 °C for 5 h (Δt = 1 °C/min, air atmosphere). Finally, the silica template was dissolved by a 2-M NaOH solution in a 50 °C water bath under continuous vigorous stirring for 24 h, then the black product was washed with distilled water and ethanol several times by centrifugation and dried at 80 °C. The template-free sample of $CoFe_2O_4$ nanocast from SBA-15 was denoted as m-$CoFe_2O_4$-1, while the sample made without etching the silica template was named $CoFe_2O_4$/SBA-1. For comparison, m-$CoFe_2O_4$-2 was also prepared under the same conditions but only for two impregnation steps. Here, the numbers '1' and '2' refer to the impregnation steps.

2.2. Material characterization

To reveal the crystallization structures of products, X-ray diffraction (XRD) measurement was performed on a Rigaku D/max-rB diffractometer with Cu-Kα radiation (λ = 1.5406 Å), in scan steps of 0.01° in a 2θ range from 10° to 90°. The morphologies and sizes of the samples were observed by a transmission electron microscope (TEM, JEOL JEM-1011). The N_2 adsorption–desorption analysis was measured on a Micromeritics ASAP 2010 instrument. The pore volumes were determined using the adsorbed volume at a relative pressure of 0.99. The multipoint BET surface area was estimated in a relative pressure range from 0.05 to 0.25. The pore size distributions of the as-prepared samples were analyzed using the Barrett–Joyner–Halenda (BJH) method. The magnetic properties were measured by a Lakeshore Model 7400 series vibrating sample magnetometer (VSM) at room temperature. The complex permeability and permittivity of the mixture were measured between 2 GHz and 18 GHz with an Agilent 8722ES network analyzer by using the transmission/reflection coaxial line method. The mesoporous $CoFe_2O_4$/paraffin (weight ratio: 3:2) composites were pressed into a toroidal shape with an outer diameter of 7 mm and inner diameter of 3 mm for microwave measurements.

3. Results and discussion

3.1. Phase, structure, and morphology characterization

Figure 1 shows the XRD patterns of serial mesoporous products. The diffraction humps centered at 23°, respectively, of $CoFe_2O_4$/SBA-1 and $CoFe_2O_4$/SBA-2 belong to the amorphous silica walls of SBA-15. While for the template-free samples (m-$CoFe_2O_4$-1 and m-$CoFe_2O_4$-2), the strong diffraction peaks can be indexed to a face-centered cubic spinel structure (JCPDS No. 22-1086). A comparison between $CoFe_2O_4$/SBA-1 and $CoFe_2O_4$/SBA-2 clearly shows that the intensity of the diffraction peak becomes stronger with the

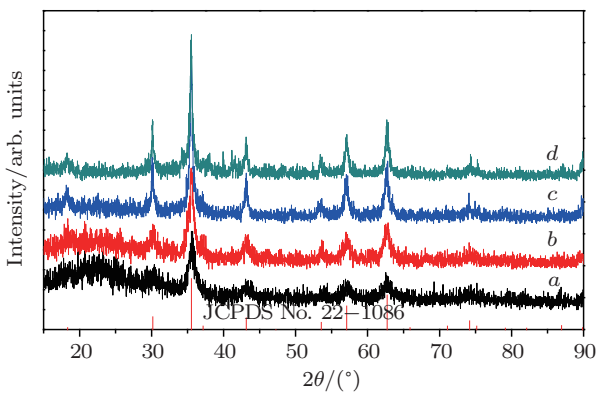


Fig. 1. (color online) X-ray diffraction patterns of (curve *a*) $CoFe_2O_4$/SBA-1, (curve *b*) $CoFe_2O_4$/SBA-2, (curve *c*) m-$CoFe_2O_4$-1, and (curve *d*) m-$CoFe_2O_4$-2.

increase of impregnation steps. After removing the template, the same phenomenon still exists.

Texture parameters of all samples were investigated by nitrogen physisorption as summarized in Table 1. The N_2 adsorption–desorption isotherms and pore size distributions for ordered mesoporous $CoFe_2O_4$/SBA and m-$CoFe_2O_4$ are given in Fig. 2. The isotherms are of type IV defined by the IUPAC classification, and they show the typical hysteresis loops of mesoporous materials prepared by the hard-templating method.[24,25]

Table 1. Textual and magnetic properties[a] of mesoporous samples.

Samples	Surface area/(m^2/g)	Pore volume/(m^3/g)	Pore size/nm	M_s/(emu/g)	M_r/(emu/g)	H_c/Oe
SBA-15	720	1.1	5.9	–	–	–
$CoFe_2O_4$/SBA-1	388.8	0.6	5.7	16.4	3.2	235.9
$CoFe_2O_4$/SBA-2	263.2	0.3	4.5	25.64	7.0	738.7
m-$CoFe_2O_4$-1	103.4	0.4	15.6	32.7	4.4	257.1
m-$CoFe_2O_4$-2	98.4	0.3	12.4	26.4	7.7	516.9

[a] Specific surface area was obtained according to BET, the pore-size distribution was derived from the adsorption branches of the isotherms using the BJH method, pore volume was estimated from the amount absorbed at a relative pressure of $P/P_0 = 0.99$, saturation magnetization (M_s), remanent magnetization (M_r), and coercivity (H_c) were measured at room temperature. The unit 1 Oe = 79.5775 A·m^{-1}.

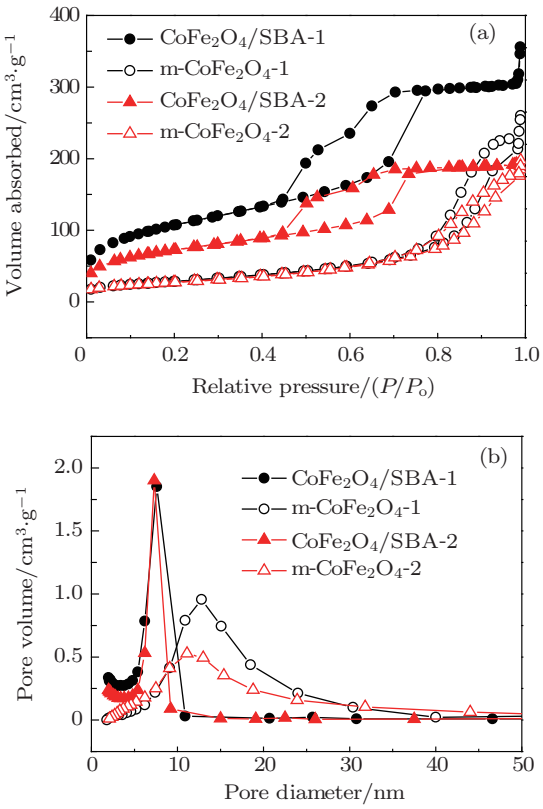


Fig. 2. (color online) N_2 adsorption–desorption isotherms (a) and pore size distributions (b) from the adsorption branches through the BJH method of the as-prepared mesoporous samples.

After the introduction of the cobalt ferrite, the surface area and the pore volume of the as-prepared sample decrease significantly, and the pore size distribution changed obviously compared with those of SBA-15. The surface areas are 388.8 m^2/g and 263.2 m^2/g, and pore volumes are 0.6 m^3/g and 0.3 m^3/g for $CoFe_2O_4$/SBA-1 and $CoFe_2O_4$/SBA-2, respectively. This is mainly attributed to the framework acting as the mesoporous silica channels during the pyrolysis and crystallization of the loaded nitrates. After removing the SBA-15, the surface area and the pore volume of the material still decrease dramatically. Both m-$CoFe_2O_4$-1 and m-$CoFe_2O_4$-2 have BET surface areas of 103.4 m^2/g and 98.4 m^2/g, and pore volumes of 0.4 m^3/g and 0.3 m^3/g respectively. It is noted that the pore size distribution shifts to a larger range, which is probably due to the existence of micropores on the amorphous silica walls of SBA-15 channels.

TEM images provide an insight into the morphologies and detailed structures of the products, and the representative images are shown in Fig. 3. Compared with pure SBA-15 (Fig. 3(a)), there obviously exist $CoFe_2O_4$ crystals in the channels of the silica template after impregnating and sintering for $CoFe_2O_4$/SBA-1 and $CoFe_2O_4$/SBA-2 as shown in Figs. 3(b) and 3(d). It is found that the loading amount of cobalt ferrite is increased with the accumulation of the impregnation step by comparing Fig. 3(b) with Fig. 3(d). This result is also in agreement with the change of surface area that decreases from 388.8 m^2/g to 263.2 m^2/g. While for template-free samples (Figs. 3(c) and 3(e)), the mesoporous structure can be still kept, and a two-step impregnation procedure is able to introduce more metal precursors into the mesopore channel and leads to a more regular structure. Therefore, the incipient wetness impregnation method was an efficient way to reduce the agglomeration of excessive cobalt ferrite on the external surface of the template.

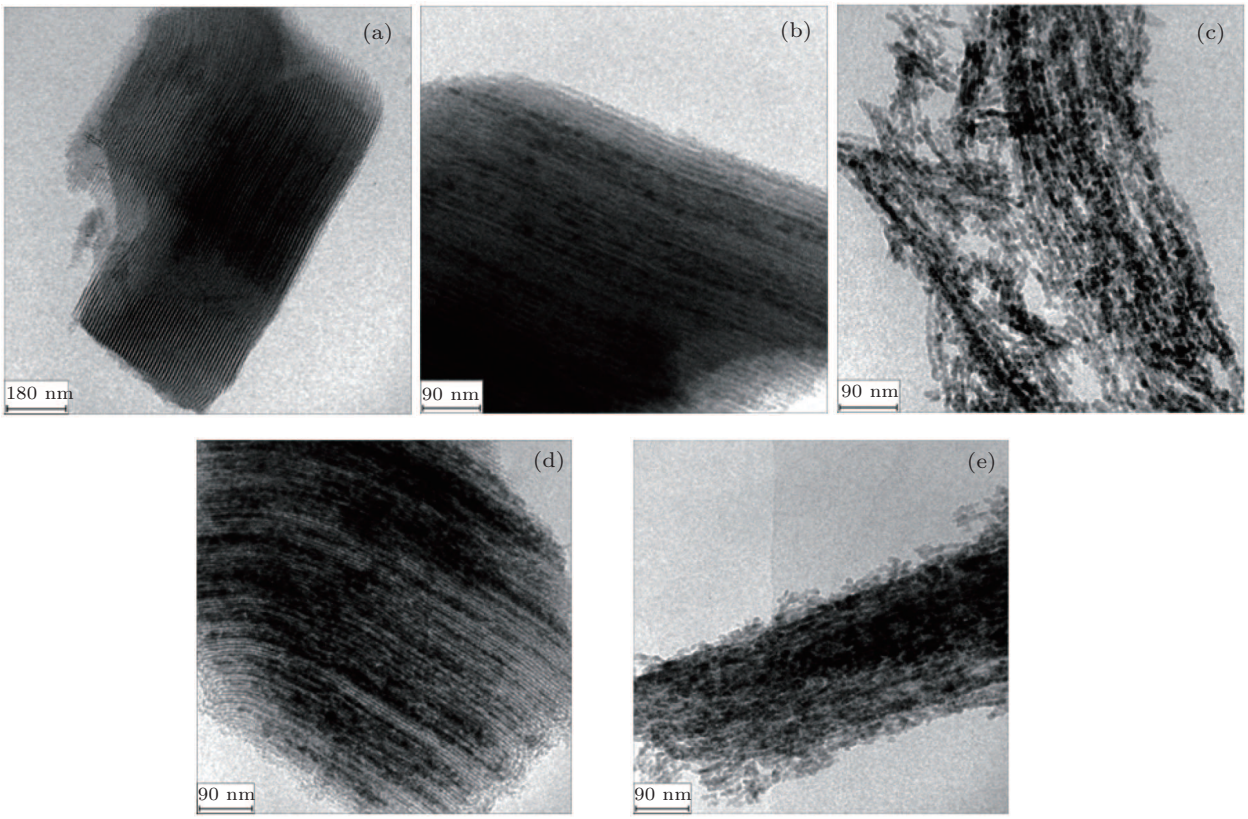


Fig. 3. TEM images of (a) SBA-15, (b) $CoFe_2O_4$/SBA-1, (c) m-$CoFe_2O_4$-1, (d) $CoFe_2O_4$/SBA-2, and (e) m-$CoFe_2O_4$-2.

3.2. Magnetic properties and microwave absorption analysis

The magnetic properties of the products were measured using a vibrating sample magnetometer at room temperature. The magnetization curves of the four samples are shown in Fig. 4. As can be seen, all the magnetization curves exhibit typical ferromagnetic behaviors.

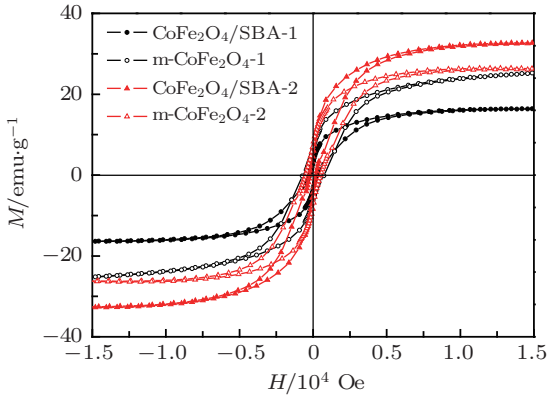


Fig. 4. (color online) Magnetic hysteresis loops of the as-prepared mesoporous samples measured at room temperature. The H unit in Oe, 1 Oe = 79.5775 A·m^{-1}.

Magnetic parameters of the four samples, obtained from the magnetization curves are also listed in Table 1. Obviously, the values of H_c and M_r of $CoFe_2O_4$/SBA-2 and m-$CoFe_2O_4$-2 are much higher than those of $CoFe_2O_4$/SBA-1 and m-$CoFe_2O_4$-1 respectively because of the more aggregated particles with the increase of impregnation time.[21] As for M_s, it tends to increase with the decrease of the sample surface area, and m-$CoFe_2O_4$-2 has the largest M_s, which benefits from its high crystallinity (Fig. 1). A large surface area will result in the noncollinear spin arrangement at or near the surface of the particle caused by breaking the exchange bond, and will give rise to a smaller M_s.[26,27] The variation of H_c is not in agreement with that of M_s, which mainly results from the differences in grain size and magnetocrystalline anisotropy.[28]

In order to investigate the microwave absorption properties of the products, the values of reflection loss (RL) of these materials were calculated using the measured complex permittivity ($\varepsilon_r = \varepsilon' - j\varepsilon''$) and complex permeability ($\mu_r = \mu' - j\mu''$). According to transmission line theory, the RL of the electromagnetic wave at the surface of a single-layer material backed by a perfect conductor at a given frequency and layer thickness can be defined with the following equations:[29,30]

$$Z_{in} = \sqrt{\frac{\mu_r}{\varepsilon_r}} \tanh\left[j\left(\frac{2\pi f d}{c}\right)\sqrt{\mu_r \varepsilon_r}\right], \quad (1)$$

$$R(\mathrm{dB}) = 20\lg\left|\frac{Z_{in}-1}{Z_{in}+1}\right|, \quad (2)$$

where d is the thickness of the absorbent, f is the frequency, c is the velocity of light, μ_r is the complex permeability, and ε_r is the complex permittivity. The RL value of -10 dB is comparable to 90% microwave absorption. In general, absorbents with an RL value less than -10 dB are considered to be suitable for electromagnetic wave absorption in theory.

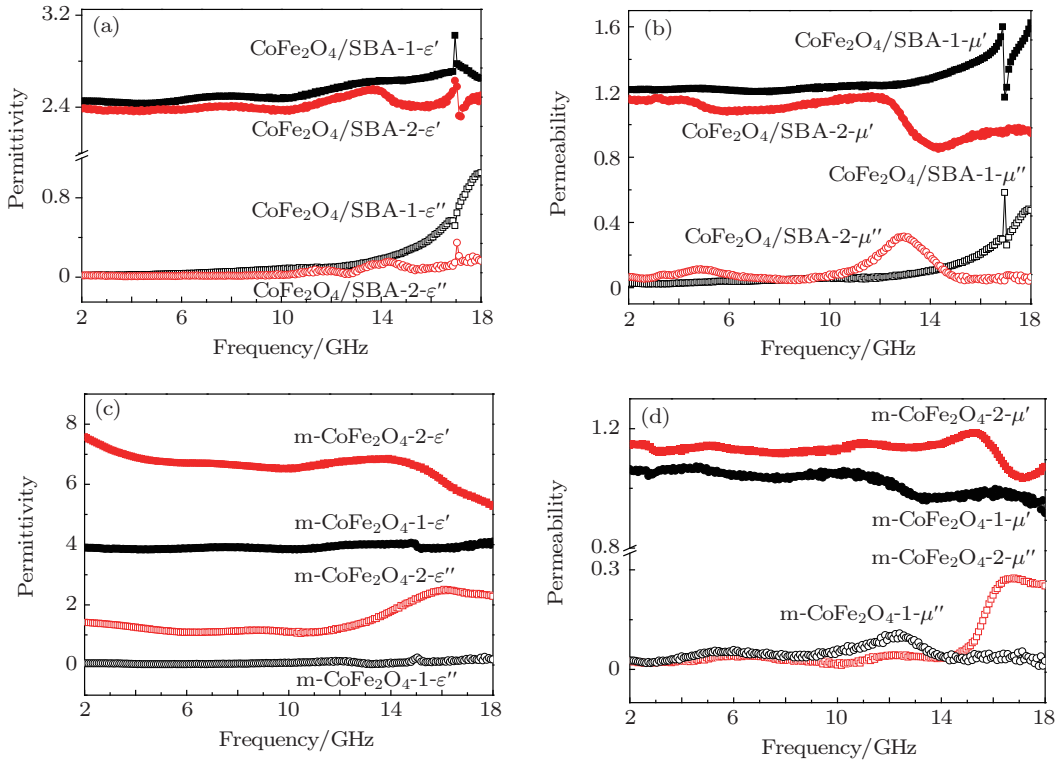


Fig. 5. (color online) Frequency dependences of the relative complex permittivity and permeability of $CoFe_2O_4$/SBA ((a) and (b)) and m-$CoFe_2O_4$ ((c) and (d)).

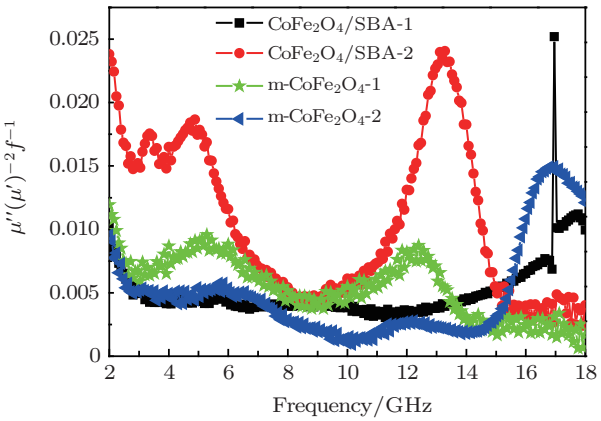


Fig. 6. (color online) Values of $\mu''\ (\mu')^{-2}f^{-1}$ of samples versus frequency.

The electromagnetic parameters of the products were investigated in a frequency range of 2 GHz–18 GHz. For the samples of $CoFe_2O_4$/SBA-1 and $CoFe_2O_4$/SBA-2, the weight ratio with paraffin is fixed at 1:4 because of their high surface area, while the ratio is 3:2 for m-$CoFe_2O_4$-1 and m-$CoFe_2O_4$-2. Figures 5(a) and 5(c) show the real part (ε') and imaginary part (ε'') of the complex permittivity respectively. It is known that ε' and ε'' represent the energy storage and dissipation capability, respectively.[31,32] For $CoFe_2O_4$/SBA-1 and $CoFe_2O_4$/SBA-2, it is noted that the values of ε' and ε'' remain almost constant in a range of 2 GHz–10 GHz, and then exhibit some fluctuations at high frequency. After removing the SBA-15, ε' and ε'' remain unchanged in the measured frequency range for $CoFe_2O_4$/SBA-1. According to the free electron theory,[33] $\varepsilon'' = 1/(2\pi\rho f\varepsilon_0)$, where ρ is the electric resistivity and ε_0 is the permittivity in a vacuum, it can be speculated that the lower ε'' means a higher electric resistivity. This eventually leads to poor microwave absorption of $CoFe_2O_4$/SBA-1 compared with that of $CoFe_2O_4$/SBA-2 (see Fig. 7).

Figures 5(b) and 5(d) display the frequency dependence of the real part (μ') and imaginary part (μ'') of complex permeability, respectively. For all the samples, the variations of μ' and μ'' are synchronous, both exhibiting the resonance peaks at high frequency. It is known that the magnetic loss of magnetic material stems mainly from exchange resonance, natural resonance, eddy current, and magnetic hysteresis loss in the microwave region.[34] In our work, the contributions of magnetic hysteresis and domain-wall resonance can be excluded due to the weak applied field, and the domain-wall resonance occurs usually in the 1 MHz–100 MHz range.[35] The eddy current loss is related to the diameter of the nanoparticle d, electric conductivity σ, and the permeability of a vacuum μ_0, which can be described by $\mu'' \approx 2\pi\mu_0(\mu')^2\sigma d^2 f/3$. If the magnetic loss only originates from the eddy current loss, the equation $\mu''(\mu')^{-2}f^{-1} = 2\pi\mu_0\sigma d^2/3$ should keep constant with changing frequency.[36] Figure 6 demonstrates the variation of $\mu''(\mu')^{-2}f^{-1}$ versus f of the samples. It is obvious that there are minor and major peaks over lower and higher frequency ranges in all curves, confirming that magnetic loss is not caused by the eddy current loss. Moreover, the obvious resonance peaks observed at high frequency in the μ'' curves may be due to the exchange resonance based on Aharoni's theory,[37,38] proven in ferromagnetic nanoparticles.

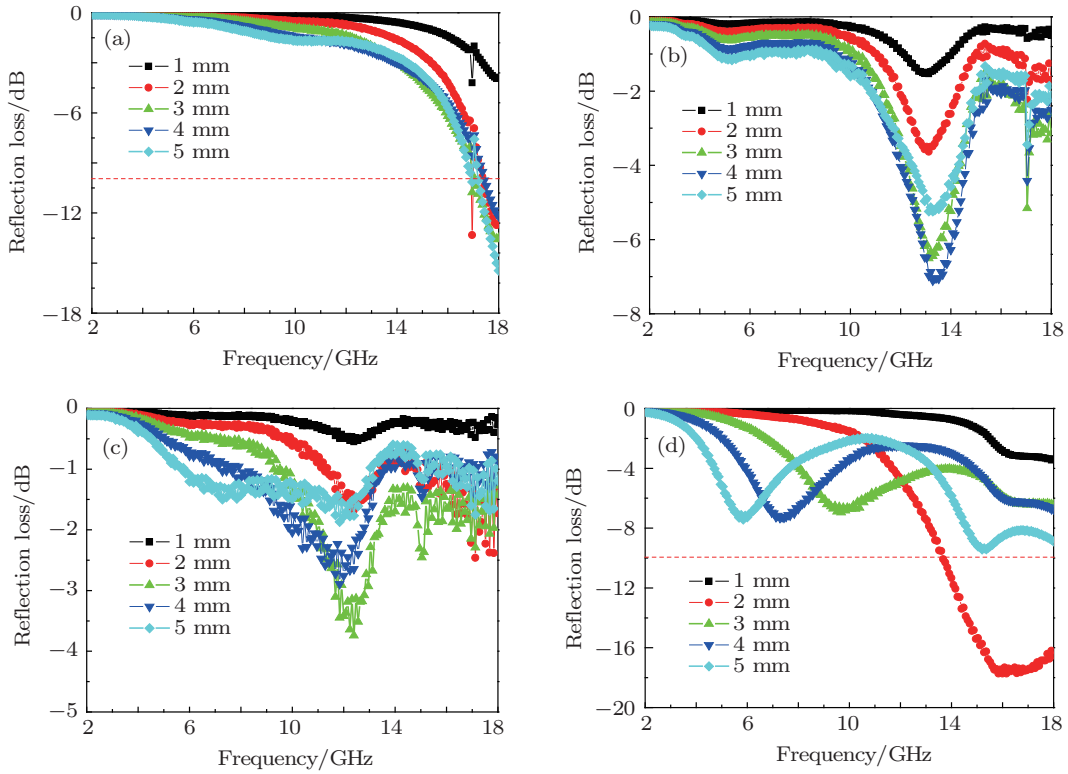


Fig. 7. (color online) Microwave RL curves of the composites with varying thicknesses in a frequency range of 2 GHz–18 GHz: (a) $CoFe_2O_4$/SBA-1, (b) $CoFe_2O_4$/SBA-2, (c) m-$CoFe_2O_4$-1, and (d) m-$CoFe_2O_4$-2.

In general, the reflection and attenuation properties of microwave absorbents depend on the matching frequency, the layer thickness of absorbent, and the complex permittivity and permeability, which are determined by their nature, shape, size, and micro-structure.[30] In order to characterize the microwave absorption properties, figure 7 shows the comparisons among calculated RL curves in the frequency range of 2 GHz–18 GHz for the product/paraffin composites with different thickness values, which are simulated based on Eqs. (1) and (2). It is evident that there is still a decreasing tendency (not shown here because of the limitation of the test instruction) of the RL curves when the frequency exceeds 18 GHz for $CoFe_2O_4$/SBA-1 and m-$CoFe_2O_4$-2. Besides, the sample of m-$CoFe_2O_4$-2 has the best microwave absorption performance, the minimum RL moves forward the lower frequency region with increasing thickness and reaches −18 dB at about 16 GHz with a thickness of 2 mm and the corresponding absorption bandwidth is 4.5 GHz (13.5 GHz–18 GHz). It is interesting to note that the matching thickness is smaller than meso-$NiFe_2O_4$ (−22.5 dB with a thickness of 3 mm) in a previous report,[13] the connected pore walls have good conductivity and the channels which exist between particles form an interface with paraffin to induce dipolar interactions and contribute significantly to the electromagnetic loss. For the samples of $CoFe_2O_4$/SBA-1 and $CoFe_2O_4$/SBA-2, the pore walls and the channels are separated by the amorphous silica walls of SBA-15, resulting in the absence of the above dipolar interactions. Therefore neither the mesoporous $CoFe_2O_4$/SBA-1 nor the $CoFe_2O_4$/SBA-2 studied here is a promising candidate for application as a light-weight microwave absorbent in the GHz range although each of them has a high surface area. The variations in both the μ' and μ'' curves of m-$CoFe_2O_4$-1 are negligibly small, indicating almost no magnetic loss contribution to the microwave absorption, and this is in agreement with the fact that it has a smaller H_c value. This is proved by Sun *et al.* via their study of dendritic Fe absorbent.[39]

4. Conclusion

In this paper, well-ordered two-dimensional mesoporous $CoFe_2O_4$ is synthesized by the nanocasting method using SBA-15 as the template with the 'two-solvent' impregnation method. Template-free m-$CoFe_2O_4$-2 shows low RL and wide absorption frequency range and proves to be a promising light-weight microwave absorbent.

References

[1] Okuno S N, Hashimoto S and Inomata K 1992 *J. Appl. Phys.* **71** 5926
[2] Zhang Z L, Wang Y H, Tan Q Q, Zhong Z Y and Su F B 2013 *J. Colloid Interf. Sci.* **398** 185
[3] Haetge J, Suchomski C and Brezesinski T 2010 *Inorg. Chem.* **49** 11619
[4] Rennard R J and Kehl W L 1971 *J. Catal.* **21** 282
[5] Xie J S, Wu Q S and Zhao D F 2012 *Carbon* **50** 800
[6] Sasmita M, Rout S R, Maiti S, Maiti T K and Panda A B 2011 *J. Mater. Chem.* **21** 9185

[7] Yang X C, Liu R J, Shen X Q, Song F Z, Jing M X and Meng X F 2013 *Chin. Phys. B* **22** 058101

[8] Meshram M R, Agrawal N K, Sinha B and Misra P S 2004 *J. Magn. Magn. Mater.* **271** 207

[9] Pullar R C, Taylor M D and Bhattacharya A K 2002 *J. Eur. Ceram. Soc.* **22** 2039

[10] Ju Y W, Park J H, Jung H R, Cho S J and Lee W J 2008 *Mater. Sci. Eng. A* **147** 7

[11] Guo P Z, Zhang G L, Yu J Q, Li H L and Zhao X S 2012 *Colloid Surf. A: Physicochem. Eng. Asp.* **395** 168

[12] Rahimi R, Kerdari H, Rabbani M and Shafiee M 2011 *Desalination* **280** 412

[13] Gu X, Zhu W M, Jia C J, Zhao R, Schmidt W and Wang Y Q 2011 *Chem. Commun.* **47** 5337

[14] Quickel T E, Le V H, Brezesinski T and Tolbert S H 2010 *Nano Lett.* **10** 2982

[15] Dahal N, Ibarra I A and Humphrey S M 2012 *J. Mater. Chem.* **22** 12675

[16] Tüysüz H, Salabas E L, Bill E, Bongard H, Spliethoff B, Lehmann C W and Schüth F 2012 *Chem. Mater.* **24** 2493

[17] Jiao F, Hill A H, Harrison A, Berko A, Chadwick A V and Bruce P G 2008 *J. Am. Chem. Soc.* **130** 5262

[18] Dickinson C, Zhou W Z, Hodgkins R P, Shi Y F, Zhao D Y and He H Y 2006 *Chem. Mater.* **18** 3088

[19] Liu S X, Yue B, Jiao K, Zhou Y and He H Y 2006 *Mater. Lett.* **60** 154

[20] Gu M, Yue B, Bao R L and He H Y 2009 *Mater. Res. Bull.* **44** 1422

[21] Sun Y Y, Ji G B, Zheng M B, Chang X F, Li S D and Zhang Y 2010 *J. Mater. Chem.* **20** 945

[22] Van der Meer J, Bardez-Giboire J, Mercier C, Revel B, Davidson A and Denoyel R 2010 *J. Phys. Chem. C* **114** 3507

[23] Zhao D Y, Huo Q S, Feng J L, Chmelka B F and Stucky G D 1998 *J. Am. Chem. Soc.* **120** 6024

[24] Zhu K K, Yue B, Zhou W Z and He H Y 2003 *Chem. Commun.* **1** 98

[25] Wang Y, Yang C M, Schmidt W, Spliethoff B, Bill E and Schüth F 2005 *Adv. Mater.* **17** 53

[26] Tung L D, Kolesnichenko V, Caruntu D, Chou N H, O'Connor C J and Spin L 2003 *J. Appl. Phys.* **93** 7486

[27] Haneda K and Morrish A H 1988 *J. Appl. Phys.* **63** 4258

[28] Poudyal N, Rong C B and Liu J P 2011 *J. Appl. Phys.* **109** 07B526

[29] Wei J Q, Zhang Z Q, Han R, Wang T and Li F S 2012 *Chin. Phys. B* **21** 037601

[30] Wang G Z, Gao Z, Tang S W, Chen C Q, Duan F F, Zhao S C, Lin S W, Feng Y H, Zhou L and Qin Y 2012 *ACS Nano* **6** 11012

[31] Atwater J E and Wheeler J R R 2004 *Appl. Phys. A* **79** 125

[32] Li G M, Wang L C, Li W X, Ding R M and Xu Y 2014 *Phys. Chem. Chem. Phys.* **16** 12390

[33] Wen F S, ZhangF and Liu Z Y 2011 *J. Phys. Chem. C* **115** 14025

[34] Ma J, Li J G, Ni X, Zhang X D and Huang J J 2009 *Appl. Phys. Lett.* **95** 102505

[35] Wu M Z, Zhang Y D, Hui S, Xiao T D, Ge S H, Hines W A, Budnick J I and Taylor G W 2002 *Appl. Phys. Lett.* **80** 4404

[36] Wen F S, Yi H B, Qiao L, Zheng H, Zhou D and Li F S 2008 *Appl. Phys. Lett.* **92** 042507

[37] Viau G, Fiévet-Vincent F, Fievet F, Toneguzzo P, Ravel F and Acher O 1997 *J. Appl. Phys.* **81** 2749

[38] Toneguzzo P, Acher O, Viau G, Fiévet-Vincent F and Fievet F 1997 *J. Appl. Phys.* **81** 5546

[39] Sun G B, Dong B X, Cao M H, Wei B Q and Hu C W 2011 *Chem. Mater.* **23** 1587